

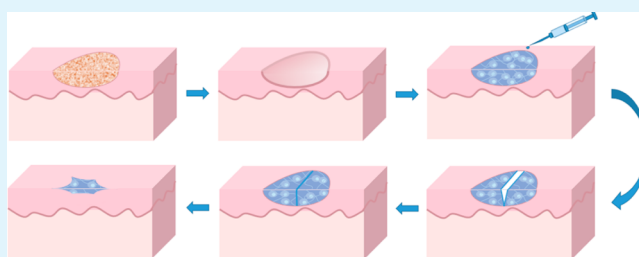
# Injectable and Self-Healing Carbohydrate-Based Hydrogel for Cell Encapsulation

Shaoyu Lü,\* Chunmei Gao, Xiubin Xu, Xiao Bai, Haogang Duan, Nannan Gao, Chen Feng, Yun Xiong, and Mingzhu Liu\*

State Key Laboratory of Applied Organic Chemistry, Key Laboratory of Nonferrous Metal Chemistry and Resources Utilization of Gansu Province and Department of Chemistry, Lanzhou University, Lanzhou 730000, People's Republic of China

**ABSTRACT:** With the fast development of cell therapy, there has been a shift toward the development of injectable hydrogels as cell carriers that can overcome current limitations in cell therapy. However, the hydrogels are prone to damage during use, inducing cell apoptosis. Therefore, this study was carried out to develop an injectable and self-healing hydrogel based on chondroitin sulfate multiple aldehyde (CSMA) and *N*-succinyl-chitosan (SC). By varying the CSMA to SC ratio, the hydrogel stiffness, water content, and kinetics of gelation could be controlled. Gelation readily occurred at physiological conditions, predominantly due to a Schiff base reaction between the aldehyde groups on CSMA and amino groups on SC. Meanwhile, because of the dynamic equilibrium of Schiff base linkage, the hydrogel was found to be self-healing. Cells encapsulated in the hydrogel remained viable and metabolically active. In addition, the hydrogel produced minimal inflammatory response when injected subcutaneously in a rat model and showed biodegradability *in vivo*. This work establishes an injectable and self-healing hydrogel derived from carbohydrates with potential applications as a cell carrier and in tissue engineering.

**KEYWORDS:** injectable hydrogel, self-healing, carbohydrate, cell encapsulation, dynamic mechanical analysis



## INTRODUCTION

Cell therapy is considered to be a very promising approach for treating various diseases. The major challenge in cell therapy is to design ideal carriers that are able to deliver therapeutic cells efficiently and specifically to the target site, avoiding the drawbacks of traditional cell therapy, such as limited cell retention, inferior cell survival, and so forth.<sup>1,2</sup> Over the past few decades, injectable hydrogels have received much attention as cell carriers.<sup>3–7</sup> Injectable hydrogels are based on a polymer solution. After administration into the body, the solution is able to gel *in situ*. Therefore, cells can be readily integrated into the hydrogel within the desired tissue to provide a local therapeutic effect, and these injectable hydrogels have the potential to mimic the extracellular matrix (ECM) and can serve to organize the cells into a three-dimensional architecture.<sup>8,9</sup> Most importantly, the injectable characteristic of the hydrogels provides homogeneous cell distribution within the desired tissue and strong adhesivity to the tissue after gelation, which increases the hydrogel-tissue interface, thereby improving the interaction of the hydrogel and host tissue.<sup>10</sup>

To be used as cell carriers, the hydrogels should show good biocompatibility, biodegradability, and nontoxicity. In light of this, natural carbohydrates have been widely explored for developing injectable hydrogels for cell delivery.<sup>11–15</sup> For example, a chitosan-Pluronic injectable hydrogel has been used to deliver bovine chondrocyte cells, showing effective chondrocyte proliferation and functional recovery for cartilage regeneration.<sup>16</sup> Chitosan-glycerol phosphate injectable hydro-

gels have been used for adipose-derived mesenchymal stem cell delivery in acute kidney injury, enhancing cell survival and improving their therapeutic effect.<sup>17</sup> A collagen-based injectable hydrogel was developed to provide facile delivery of retinal pigment epithelial (RPE) cells into the eye to treat retinal degenerative diseases.<sup>18</sup> Recently, Lee et al. found that incorporation of type-II collagen or chondroitin sulfate into chitosan injectable hydrogels further increased proliferation and cartilage matrix production by encapsulated chondrocytes and mesenchymal stem cells (MSCs).<sup>19</sup> These natural carbohydrates have shown good biocompatibility and also promote cell survival and proliferation. However, although great effort has been put forth to prepare injectable hydrogels for cell encapsulation, the development of real systems used in clinical applications is still in its incipient stage. The reason for this lies in the possible toxicity of the agents used, undesirable side effects from gel degradation, the complex synthesis process, and the high cost of the systems.

Considering the parameters described above, we developed an injectable hydrogel based on natural polymer chondroitin sulfate and chitosan. Chondroitin sulfate is the major glycosaminoglycan (GAG) that is abundant in the extracellular matrix of tissues. It has many attractive properties, such as hydrophilicity, biocompatibility, and biodegradability.<sup>20,21</sup> In addition, chondroitin sulfate can influence cell biological responses, which are

Received: April 11, 2015

Accepted: May 28, 2015

Published: May 28, 2015

useful in tissue repair and regenerative medicine applications.<sup>22</sup> Chitosan is another attractive base material for medical and pharmaceutical applications due to its biocompatibility, biodegradability, and stimulation of cellular activities.<sup>23</sup> Despite a few examples of injectable hydrogels based on chondroitin sulfate and/or chitosan, the complicated synthetic procedures (e.g., photo-cross-linking,<sup>19,24</sup> enzymatic cross-linking,<sup>25</sup> grafting reactions,<sup>15,26,27</sup> and click chemistry<sup>28</sup>) and the potential cytotoxicity of the agents used (e.g., photoinitiator, a local high concentration of H<sub>2</sub>O<sub>2</sub> in the peroxidase-catalyzed cross-linking systems) impede their applications. Herein, we develop an injectable hydrogel using *N*-succinyl-chitosan and chondroitin sulfate through an inexpensive, facile, and fast method. Chondroitin sulfate was oxidized with sodium periodate by cleaving the vicinal glycols to obtain multiple aldehyde groups, enabling chondroitin sulfate to serve as a macromolecular cross-linker for *N*-succinyl-chitosan to formulate hydrogels. Hydrogels were formed by self-cross-linking without using any cross-linking agents. In addition, the hydrogels were found to be self-healing under physiological conditions without any external stimulus. As far as we know, there are few carbohydrate-based self-healing injectable hydrogels reported.

Self-healing injectable hydrogels can be obtained through selective metal–phosphate interactions,<sup>29</sup> supramolecular interactions,<sup>30</sup> or dynamic covalent linkage.<sup>31</sup> Among these, Schiff-base-formed hydrogels are of great interest because gelation and healing readily occurred at physiological conditions without requiring other stimuli.<sup>32</sup> Additionally, Schiff-base-based hydrogels are promising because carbohydrates can be modified using facile approaches to obtain aldehydes and amine groups. In this work, we focused on the ability of carbohydrates of chondroitin sulfate and chitosan to form self-healing injectable hydrogels. The self-healing property of the injectable hydrogels allows the autonomic healing to repair damage that occurs during use. For hydrogels used in cell therapy, the damage would induce undesirable diffusion of cells to the surrounding tissues and make cells undergo apoptosis in the harsh ischemic environment. In addition, the damage could cause migration and/or degradation of in situ forming hydrogels.<sup>33</sup> From these perspectives, carbohydrate-based injectable hydrogels capable of repairing damage autonomously have become an area of particular scientific and commercial interest.

## EXPERIMENTAL SECTION

**Materials.** Chondroitin sulfate (molecular weight of 72,000) was obtained from Shanghai Sangon Biological Engineering Technology & Services Co., Ltd. (Shanghai, China). Chitosan (molecular weight of 270,000, deacetylation degree of 90.8%) was supplied by Golden-Shell Biochemical Co., Ltd. (Zhejiang, China). Other chemicals were analytical grade and used without further purification.

**Synthesis of Chondroitin Sulfate Multiple Aldehyde (CSMA).** Chondroitin sulfate (1 g) was dissolved in 100 mL of water, and then 0.27 g of sodium periodate (in 5 mL of water) was added. The mixture was stirred in the dark at room temperature for 2 h to obtain CSMA. Then, 1 mL of diethylene glycol was added to inactivate the unreacted periodate. Then, the product was dialyzed against water for 3 days and freeze-dried using a Labconco freeze-dryer. The oxidation degree of CSMA is the oxidized glucuronic acid residue number per 100 glucuronic acid units and quantified by TNBS assay.<sup>34</sup>

**Synthesis of *N*-Succinyl-Chitosan (SC).** A 2% solution of chitosan in lactic acid (5%) was prepared, and then 60 mL of methanol was added. Into this chitosan-methanol solution was dissolved 3 g of succinic anhydride, and the mixture was stirred constantly for 1 day at room temperature. Thereafter, the product was isolated by precipitation into a KOH-ethanol solution and then redissolved in water. The solution was

dialyzed extensively against water for 3 days and freeze-dried. The substitution degree of SC was measured by ninhydrin.<sup>35</sup>

**Preparation of CSMA/SC Injectable Hydrogels.** CSMA and SC were dissolved in phosphate buffered saline (PBS, pH 7.4, 0.1 M) separately at a concentration of 30 mg/mL. Then, each polymer solution was mixed and loaded into a syringe. Then, the CSMA/SC hydrogel precursor was injected into a round Teflon mold to form the gel. The mole ratio of aldehyde to amine was controlled at 2:4, 3:3, and 4:2. The final hydrogels were marked as CSMA2/SC4, CSMA3/SC3, and CSMA4/SC2, respectively. The gelation time of the hydrogels was determined using a previously reported method.<sup>36</sup>

**Characterization.** Fourier transform infrared (FTIR) spectroscopy of chondroitin sulfate, CSMA, chitosan, SC, and CSMA/SC hydrogels was performed on a Nicolet NEXUS 670 FTIR spectrometer using the KBr pellet method. The morphology of the hydrogels was determined using scanning electron microscopy (SEM). The prepared hydrogels were quickly frozen in liquid nitrogen and then lyophilized using a Labconco freeze-dryer for 12 h. Then, the samples were sputtered with gold and examined using a JSM-5600LV SEM (Japan).

**Determination of Cross-Linking Density and Molecular Weight between Cross-Links of CSMA/SC Injectable Hydrogels.** Cross-linking density ( $\nu$ , mol/cm<sup>3</sup>) of the hydrogels was calculated from the Flory–Rehner equation<sup>37</sup>

$$\nu = \frac{-[\ln(1 - \nu_2) + \nu_2 + \chi_1 \nu_2^2]}{\nu_1 \left( \nu_2^{1/3} - \frac{\nu_2}{2} \right)} \quad (1)$$

where  $\chi_1$  is the interaction parameter of water and the polymer (CSMA/SC), which was assumed to be 0.35,<sup>38</sup>  $\nu_1$  is the molar volume of water (18.062 cm<sup>3</sup>/mol), and  $\nu_2$  is the polymer (CSMA/SC) volume fraction in the equilibrium-swollen hydrogel.

The  $\nu_2$  value can be calculated using eqs 2–4

$$\nu_2 = \frac{\nu_p}{\nu_{g,s}} \quad (2)$$

$$\nu_p = \frac{W_{a,r}}{\rho_p} \quad (3)$$

$$\nu_{g,s} = \frac{W_{a,s} - W_{n,s}}{\rho_n} \quad (4)$$

where  $\nu_p$  and  $\nu_{g,s}$  are the volume of the unswollen and swollen hydrogel, respectively,  $W_{a,r}$  is the weight of dry hydrogel in air,  $W_{a,s}$  and  $W_{n,s}$  are the weight of the swollen hydrogel in air and in *n*-heptane (nonsolvent for CSMA/SC), respectively, and  $\rho_p$  and  $\rho_n$  are the density of the polymer (CSMA/SC, 1.164 g/cm<sup>3</sup>) and *n*-heptane (0.659 g/cm<sup>3</sup>), respectively.

The molecular weight between cross-links in polymer  $M_c$  was calculated by dividing the polymer density  $\rho_p$  by  $\nu$ .

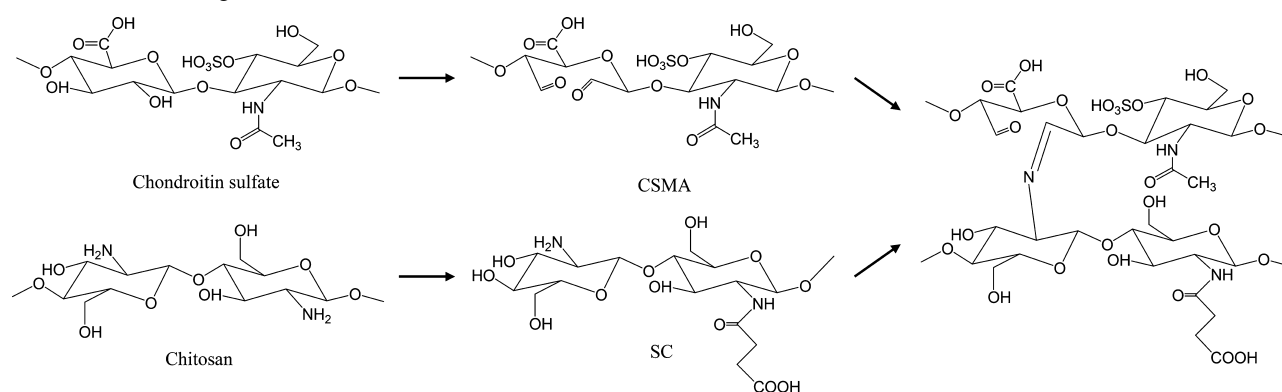
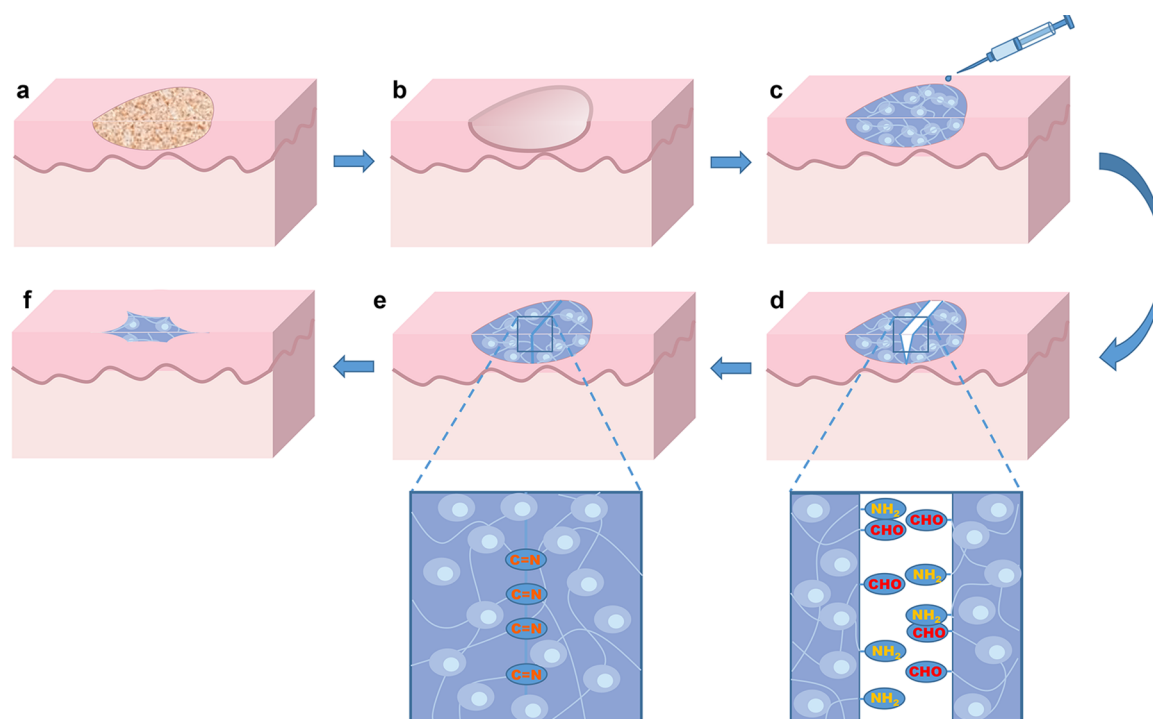
**Water Content of CSMA/SC Injectable Hydrogels.** For the water content measurements, the hydrogels were vacuum-dried to obtain a constant weight and then immersed in distilled water at 37 °C. Swollen gels were removed from water at determined intervals and weighed until equilibrium was reached. The water content of the hydrogels was calculated using the equation

$$\text{Water Content} = \frac{W_e}{W_d} \times 100\% \quad (5)$$

where  $W_e$  and  $W_d$  are the weights of the equilibrium-swollen and dry gels, respectively.

**Mechanical Properties of CSMA/SC Injectable Hydrogels.** The storage modulus  $G'$  and the loss modulus  $G''$  of the hydrogels were determined by dynamic mechanical analysis (DMA). The hydrogels were cut into cylinders with a height of 1 mm and diameter of 10 mm, and then measured at 25 °C using a dynamic mechanical analyzer (DMA/SDTA861e, Mettler Toledo, Switzerland). The frequency sweep was performed over a frequency range of 0.01–100 Hz at a strain of 1%.

Scheme 1. Scheme of Molecular Modification of Chondroitin Sulfate and Chitosan and the Hydrogel Formation Mechanism via the Schiff's Base Linkage

Scheme 2. Scheme of the CSMA/SC Injectable and Self-Healing Hydrogel Used as Cell Carriers for Tissue Repair<sup>a</sup>

<sup>a</sup>(a) Lesion on soft tissue. (b) Pathological tissue is removed. (c) Cells are encapsulated in CSMA/SC gel precursors and injected subcutaneously by a syringe. (d) CSMA/SC hydrogel is formed in situ and damaged under a variety of environmentally and therapeutically relevant stressors, such as impressed forces, body fluids, and any chemical and bioactive species available. (e) CSMA/SC hydrogel heals itself automatically without additional stimuli. Self-healing is achieved through dynamic imine bonds between amino groups on SC and aldehyde groups on CSMA. (f) Following delivery of therapeutic cells to the target tissue, the CSMA/SC hydrogel is biodegraded and replaced by normal tissue.

#### Self-Healing Behavior of CSMA/SC Injectable Hydrogels.

CSMA3/SC3 hydrogels were prepared in a round Teflon mold and then aged in the mold at room temperature for 3 h. As a comparison, one of the hydrogels was stained with curcumin. Then, two hydrogels were spliced and placed in a container with moisture at room temperature without any other intervention for 2 h to heal completely. Then, the hydrogels were drawn by tweezers, and pictures were taken. The morphology of the healed hydrogel was determined using SEM after lyophilization.

**Cell Encapsulation of CSMA/SC Injectable Hydrogels.** Before encapsulation, HeLa cells were mixed with 20  $\mu$ M Dio and incubated at 37  $^{\circ}$ C for 30 min. After the dye was removed, the cells were cultured in DMEM with 10% of fetal bovine serum (FBS) containing 100 units/ml of penicillin/streptomycin. CSMA and SC were sterilized under UV irradiation for 1 h and then dissolved in sterilized PBS. Then, HeLa cells were mixed with sterilized SC solutions. The HeLa/SC solution was

pipetted into a Petri-dish, and the CSMA solution in DMEM media was then pipetted into the same dish and gently mixed to form the hydrogel, organizing the cells into a three-dimensional architecture. All encapsulation studies were performed with  $1 \times 10^5$  cells/200  $\mu$ L of culture medium in each 60  $\mu$ L hydrogel precursor. Varying concentrations of CSMA/SC hydrogels were determined. For reference purposes, cells where no CSMA/SC hydrogels were added to the medium were taken as a control. At regular intervals, cell viability was determined by MTT assay, and fluorescent images were taken. Confocal microscopy (FluoView FV1000MPE, OLYMPUS) was used to determine the distribution of cells within the hydrogels.

**In Vivo Degradation of CSMA/SC Injectable Hydrogels.** Male rats (~200 g) were used for in vivo degradation studies. The rats were acclimated for 1 week before experiments. All care and handling of the animals were performed with the approval of the Institutional Authority for Laboratory Animal Care. Anesthesia was induced with a 3% sodium

pentobarbital solution. The abdominal region of the rats was shaved, and then 0.5 mL of the CSMA/SC mixture aqueous solution (3 wt %) was injected subcutaneously by a syringe with a 21-gauge needle. The diameter of the hydrogel formed was measured every week for 7 weeks. At designated time intervals (1 day, 3 weeks, and 7 weeks), the rats were sacrificed, and the injection site was carefully cut open and photographed. The surrounding tissues were surgically removed, and the inflammatory responses in the rats were examined using hematoxylin and eosin (H&E) stains.

## RESULTS AND DISCUSSION

**Preparation of CSMA/SC Injectable Hydrogels.** Periodate breaks the vicinal glycols on the glucuronic acid unit of chondroitin sulfate, forming multiple aldehyde groups (Scheme 1). The obtained CSMA has an oxidation degree of 54.6% as determined by a TNBS assay. Its molecular weight is determined to be 45,000, which is much lower than that of chondroitin sulfate, indicating the polymer was cleaved during the oxidation. SC was obtained by introducing succinyl groups to the N-terminal of the glucosamine units on chitosan, rendering chitosan soluble in water. Its substitution degree is determined to be 48.1%. Hydrogels are rapidly formed by mixing CSMA and SC aqueous solutions. Hydrogels are formed mainly due to Schiff base reactions because of the existence of abundant aldehyde groups along the CSMA molecular chains in conjunction with the plentiful amino groups on SC (Schemes 1 and 2). In addition, physical cross-linking (e.g., hydrogen bonding and chain entanglements) also reinforces the network formed by chemical cross-linking.

Gelation time is vital for injectable hydrogels because fast gelation would induce hydrogel formation before injection, whereas slow gelation would result in gel precursors diffusing away from the injection site.<sup>39</sup> In this study, the gelation time of the CSMA/SC injectable hydrogels is  $41 \pm 6$ ,  $29 \pm 4$ , and  $34 \pm 3$  s for CSMA2/SC4, CSMA3/SC3, and CSMA4/SC2, respectively. It is noted that CSMA3/SC3 has the fastest gelation rate. It is calculated that the aldehyde concentrations of CSMA and the amino groups of SC are 69 and 87 mM, respectively. Therefore, the theoretical  $[\text{CHO}]/[\text{NH}_2]$  ratio is approximately 1:1 for equal volumes of CSMA and SC. The highest cross-linking density is thus achieved for CSMA3/SC3, which facilitates the fastest gel formation.

**Characterization.** Figure 1 shows the FTIR spectra of chondroitin sulfate, CSMA, chitosan, SC, and CSMA/SC hydrogels. In the spectrum of chondroitin sulfate (Figure 1a), some characteristic peaks can be ascribed at  $1655 \text{ cm}^{-1}$  for amide bands,  $1257 \text{ cm}^{-1}$  for S=O stretching vibration,  $1416$  and  $1379 \text{ cm}^{-1}$  for the coupling of the C–O stretching vibration and O–H variable-angle vibration of –COOH. In the CSMA spectrum (Figure 1b), a peak appears at  $1745 \text{ cm}^{-1}$ , which is due to aldehyde symmetric vibrations. A previous study reported that hemiacetals formed between aldehyde groups of hexuronic acid and hydroxyl groups of unoxidized residues.<sup>40</sup> This could explain why the peak of aldehyde is inconspicuous. Other studies reported similar results.<sup>41,42</sup> In the chitosan spectrum (Figure 1c), the peak at  $1599 \text{ cm}^{-1}$  corresponds to the bending vibration absorption of amino groups. The characteristic bands of the chitosan saccharine structure are found at  $1156 \text{ cm}^{-1}$  (C–O–C asymmetric stretching),  $1087$ , and  $1032 \text{ cm}^{-1}$  (skeletal vibration involving the C–O stretching). It is noted that three bands at  $1567$ ,  $1654$ , and  $1406 \text{ cm}^{-1}$  become broader in the spectrum of SC (Figure 1d), which are attributed to –NH– bending vibration, amide I, and amide III, respectively, suggesting substitution of the chitosan. In the spectrum of the CSMA/SC

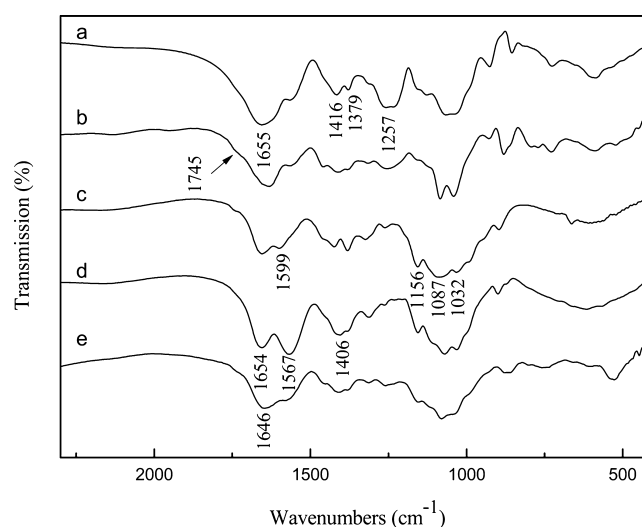


**Figure 1.** FTIR spectra of chondroitin sulfate (a), CSMA (b), chitosan (c), SC (d), and the CSMA3/SC3 hydrogel (e).

hydrogel (Figure 1e), a band at  $1646 \text{ cm}^{-1}$  is detected, which is the characteristic band of the imine structure (–C=N–), indicating that a Schiff base reaction has occurred.

The network architecture of the hydrogel is directly correlated with water content, which affects the transportation of nutrients and oxygen. The interior morphology of the hydrogels was investigated by SEM, and the results are shown in Figure 2. The

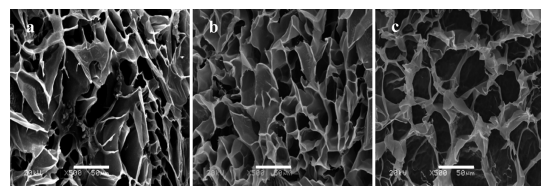


**Figure 2.** SEM images of CSMA/SC hydrogels (a) CSMA2/SC4, (b) CSMA3/SC3, and (c) CSMA4/SC2. Scale bar = 50  $\mu\text{m}$ .

morphology suggests that the interior structure of the hydrogel is dependent on the hydrogel composition. CSMA3/SC3 (Figure 2b) shows the smallest pore diameters and tightest network structure relative to CSMA2/SC4 (Figure 2a) and CSMA4/SC2 (Figure 2c), which may be due to comparatively sufficient cross-linking. According to Figure 2, all of the hydrogels display a continuous and porous three-dimensional structure. This interconnected porous structure provides adequate void space for cell proliferation as well as oxygen and nutrient transportation. The microstructure and high water content (see Water Content section) are similar to that of the extracellular matrix of natural tissue,<sup>43</sup> allowing the hydrogel to support cell encapsulation and survival.

**Cross-Linking Density and Molecular Weight between Cross-Links.** The crucial structural parameters characterizing the cross-linked hydrogels are the cross-linking density ( $\nu$ ) and the molecular weight between cross-links ( $M_c$ ). The cross-linking density represents the fraction of units involved in the cross-linking and provides the possibility of quantitatively determining the random cross-linked structure of a network. The molecular weight between cross-links is the average molecular weight of the polymer chains between chemical and physical cross-linked points. These parameters provide a measurement of the cross-linking degree in the hydrogels. In the present study,  $\nu$  and  $M_c$  of

the CSMA/SC hydrogels were estimated and shown in Table 1. As expected, CSMA3/SC3 shows the highest cross-linking

**Table 1. Water Content, Cross-Linking Density ( $\nu$ ), and Molecular Weight between Cross-Links ( $M_c$ ) of CSMA/SC Hydrogels**

sample	water content (g/g)	$\nu$ ( $\times 10^3$ , mol/cm <sup>3</sup> )	$M_c$ (g/mol)
CSMA2/SC4	14.1	0.12	9511.54
CSMA3/SC3	22.8	1.13	1026.67
CSMA4/SC2	60.1	0.50	2329.09

density and lowest molecular weight between cross-links relative to those of CSMA2/SC4 and CSMA4/SC2. In this study, the CSMA/SC hydrogel network is formed by the cross-linking of  $-\text{CHO}$  of CSMA and  $-\text{NH}_2$  of SC; therefore, chemical cross-linking density is closely related to the concentrations of the aldehyde of CSMA and the amino groups of SC. For CSMA3/SC3, the theoretical  $[\text{CHO}]/[\text{NH}_2]$  ratio is approximately 1:1; therefore, the highest cross-linking density is achieved among the three CSMA/SC ratios. In the other two formulations, either aldehyde groups or amino groups are in relative excess. It is noted that the content of aldehyde groups of CSMA is slightly lower than that of amino groups of SC. Therefore, it is understandable that CSMA4/SC2 with more CSMA will yield a higher cross-linking density than that of CSMA2/SC4.

**Water Content.** The water content of CSMA/SC hydrogels at 37 °C was examined and shown in Table 1. From the table, we can see that all of the hydrogels have high water content because both CSMA and SC have many hydrophilic groups, such as hydroxyl, carboxyl, and amino groups, which contribute to the great hydration capacity and lead to a high water content. The high water content will promote the exchange of ions, nutrients, and metabolites with the fluids of the surrounding tissue, maintaining the viability and proliferation of the encapsulated cells.<sup>1</sup>

Table 1 illustrates the effect of network composition on the water content of the hydrogel. As mentioned before, CSMA3/SC3 has the highest cross-linking density. Therefore, one would expect the lowest water content to be obtained for CSMA3/SC3. However, this was not evident in the water content studies. The

data in Table 1 show that a higher cross-linking density is not associated with lower water content. A similar phenomenon was observed by other researchers.<sup>21,34</sup> The reason for the present case is that chondroitin sulfate plays an important role in water content of the hydrogels. As we know, there are many carboxylate and sulfate groups in the chondroitin sulfate chains, which have better hydrophilic ability than hydroxyl and amino groups in SC. In addition, electrostatic repulsion between the negatively charged carboxylate and sulfate groups further expands the network. This results in increased water content with an increase in CSMA content in the hydrogels.

**Mechanical Properties.** The mechanical properties of CSMA/SC hydrogels were determined by a DMA in shear mode. The storage modulus  $G'$  and loss storage  $G''$  were presented as functions of frequency at a fixed strain ( $\gamma$ ) of 1%, as shown in Figure 3.  $G'$  represents the elastic part of the hydrogel, whereas  $G''$  corresponds to the viscous part. From the figure, it can be seen that all of the hydrogels display an elastic characteristic with  $G'$  higher than  $G''$  at a high frequency region. At low frequencies, however,  $G''$  dominates  $G'$  for CSMA2/SC4 at angular frequencies below 0.015 rad/s, at which point  $G'$  crosses over  $G''$ . Typically, hydrogels formed by covalent bonds display frequency-independent dynamic rheology behavior (i.e.,  $G'$  and  $G''$  are frequency-independent with  $G' > G''$ ). However, for hydrogels containing reversible bonds, frequency-dependent moduli are observed, which is because there is enough time for the kinetically labile cross-links to regenerate at low frequencies. At high frequencies, the time scale is not sufficiently long for the labile cross-links to dissociate, and elastic-like behavior dominates, showing frequency-independent behavior with  $G' > G''$ .<sup>44</sup> However, for CSMA3/SC3,  $G'$  displays a frequency independent plateau, and  $G'$  is much higher than  $G''$  during the entire frequency range of 0.01–100 Hz. This demonstrates that the hydrogels with the highest cross-linking density behave like a permanently cross-linked hydrogel network. Furthermore, it is noted that  $G'$  of CSMA3/SC3 is significantly greater than that of the other hydrogels, demonstrating that CSMA3/SC3 could store more energy than its counterparts formulated using the other two ratios. As stated previously, the theoretical  $[\text{CHO}]/[\text{NH}_2]$  ratio is approximately 1:1 for CSMA3/SC3. Therefore, more imine bonds are formed, resulting in a stiffer network as

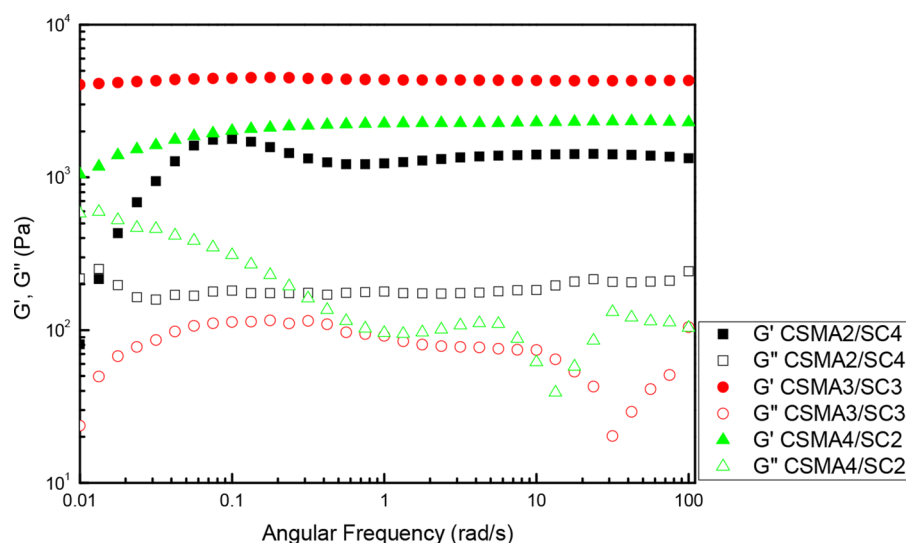


**Figure 3.** Storage modulus  $G'$  and loss storage  $G''$  of CSMA/SC hydrogels as a function of frequency at a fixed strain ( $\gamma$ ) of 1%.

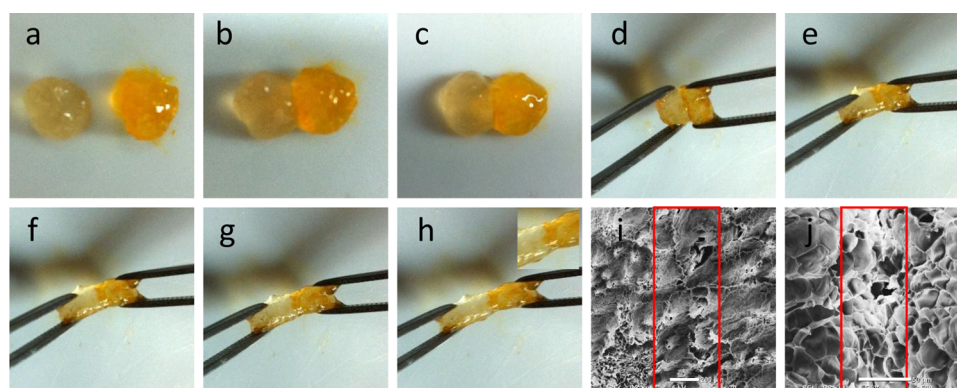


**Figure 4.** Self-healing behavior of the CSMA3/SC3 hydrogel. (a) CSMA3/SC3 hydrogels prepared in a round Teflon mold. One of the hydrogels is dyed yellow to allow for an easily distinguishable interface. (b) Two hydrogels are spliced and placed in a container with moisture at room temperature without any other intervention. (c) The hydrogels healed in 2 h. (d–h) The hydrogels are stretched by tweezers, illustrating the weld-line strength. (i, j) SEM images of the healed hydrogel. (i): surface,  $\times 70$ , scale bar =  $200\ \mu\text{m}$ ; (j): internal,  $\times 500$ , scale bar =  $50\ \mu\text{m}$ .

evidenced by the higher storage modulus. The storage modulus of the hydrogel improved when the cross-linking density increased, as other studies have reported. However, this is the first study that determines the mechanical properties of an injectable, self-healing hydrogel under dynamic conditions. We believe that determining the mechanical properties of the hydrogel under dynamic conditions would be important when applying the injectable, self-healing hydrogel to a dynamic tissue, such as cartilage.

It has been demonstrated that cell fate and cell behavior can be strongly influenced by the stiffness of biomaterials.<sup>22,45</sup> Banerjee et al. studied the influence of the mechanical properties of alginate hydrogels on the proliferation and differentiation of neural stem cells (SCs). They found that the proliferation rate of SCs decreased when the modulus of the hydrogels increased. In addition, SCs differentiation into neurons was favored within hydrogels with an elastic modulus similar to brain tissue.<sup>46</sup> The mechanical properties being comparable to soft tissue can minimize foreign material/tissue mismatch. Therefore, control over the hydrogel mechanical properties would be advantageous. It is well-known that many of the macroscopic properties of hydrogels, including mechanical properties, are dependent on the cross-linking density. In general, a greater extent of cross-linking density typically produces more stable hydrogels. This is likely due to a high degree of intramolecular cross-linking at high cross-linking density. Thus, cross-linking density can be used to control the mechanical properties of the hydrogel. In this study, the mechanical properties of the hydrogels can be tuned to mimic soft tissues by changing the molar ratio of CSMA and SC. Therefore, we can develop mechanically tunable soft supports for cell culture based on CSMA and SC.

**Self-Healing Property.** The self-healing property based on the dynamic chemistry of Schiff base was studied. CSMA3/SC3 hydrogels were prepared; one of which was stained with curcumin (Figure 4a). Upon placing two hydrogels close together in a container in air saturated with moisture, they can heal autonomously in 2 h. As shown in Figure 4, the two hydrogels merged into a single one with a stronger junction point, which could not be stretched or broken. The hydrogel is formed through dynamic imine linkage between aldehyde groups on CSMA and amino groups on SC, and the cleavage and regeneration of the imine bonds continuously occurs in the hydrogel. Therefore, the hydrogel could heal itself automatically without additional stimuli. In addition, physical cross-linking,

mostly due to hydrogen bonds and chain entanglements, also reinforces the network formed by imine bonds. SEM pictures also support the idea that the two hydrogels merged into a single one as the network connected together, although the seam was still visible (Figure 4i and j).

Hydrogels are prone to damage under a variety of environmentally and therapeutically relevant stressors, such as impressed forces, body fluids, and any available chemical and bioactive species. For hydrogels used as cell delivery carriers, the damage would induce undesirable diffusion of cells to the surrounding tissues and make cells undergo apoptosis in the harsh ischemic environment. In addition, the damage could cause migration and/or degradation of in situ forming hydrogels. The self-healing property of the CSMA/SC hydrogels allows autonomic healing to repair these damages, providing a microenvironment for cell proliferation and a mechanical support for the target tissue.

**Cell Encapsulation.** The cell viability, together with the distribution, are important aspects to take into account when determining the potential of the CSMA/SC hydrogel as a cell delivery vehicle. Evaluating the cell viability after encapsulating in the hydrogels was performed by MTT assay, and the results are shown in Figure 5. It can be seen that incubation of HeLa cells

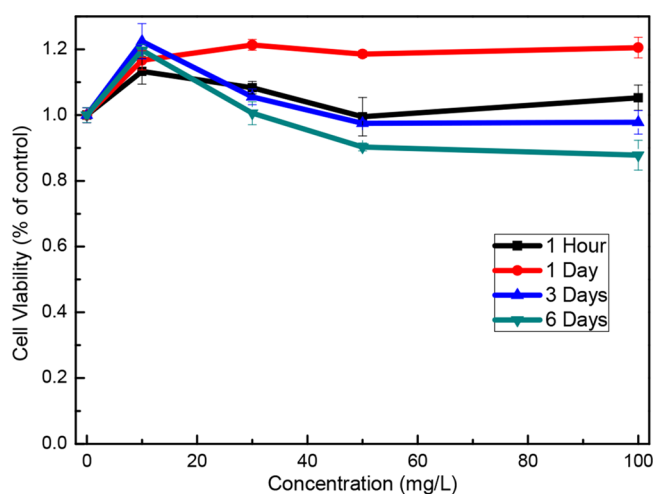


**Figure 5.** HeLa cells were encapsulated in CSMA3/SC3 hydrogels with varying concentrations for 1 h, 1 day, 3 days, and 6 days, and viability was quantified using MTT assays. Values are normalized to controls (cells without hydrogel).

with varying concentrations of CSMA3/SC3 hydrogels for three days did not appear to have any significant deleterious effect on cell viability. However, after six days of incubation *in vitro*, viability of cells incubated with hydrogels decreased more than that of control samples ( $p = 0.8$ ), which may be because oxygen and metabolite diffusion became limited with the increased cell density. It is noted that there was a marked increase in cell number after one day of cell culture in the three-dimensional environment of the hydrogels, demonstrating that the hydrogels provided an adequate environment for living cells. The fluorescent images also show a significant increase in cell numbers, which indicates that cells were able to proliferate in the hydrogel (Figure 6). Cell distribution within the hydrogels was

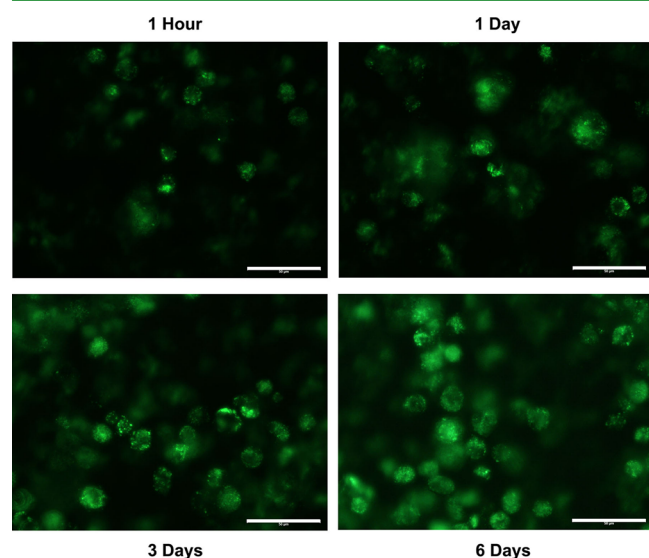


**Figure 6.** Fluorescent images of cells stained by Dio after culture with CSMA3/SC3 hydrogels (30 mg/L) for 1 h, 1 day, 3 days, and 6 days. Scale bar = 50  $\mu\text{m}$ .

examined by confocal microscopy during the *in vitro* culture, as shown in Figure 7. Z-scans reveal that the cells were distributed at different depths throughout the whole hydrogel from top to bottom (I–VI). This demonstrates the ability of the hydrogel to efficiently entrap cells. These results suggest that cells retained their proliferative capacity in the hydrogel microenvironment

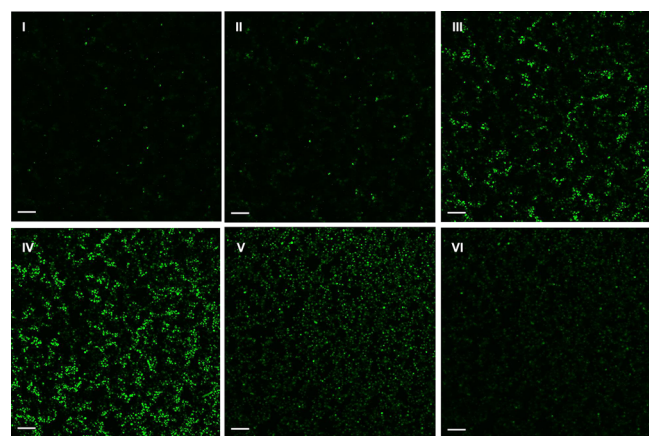


**Figure 7.** Confocal images of HeLa cells stained by Dio when incubated with CSMA3/SC3 hydrogels (30 mg/L). Z-scans show the distribution of cells from top to bottom (I–VI). Scale bar = 100  $\mu\text{m}$ .

and that the hydrogel can be used as a vehicle for the delivery of therapeutic cells.

**In Vivo Degradation.** Following delivery of therapeutic cells to the target site, it would be beneficial if the hydrogel is degraded and replaced by normal tissue. Thus, *in vivo* biodegradation of the CSMA/SC injectable hydrogels was determined. Figure 8a

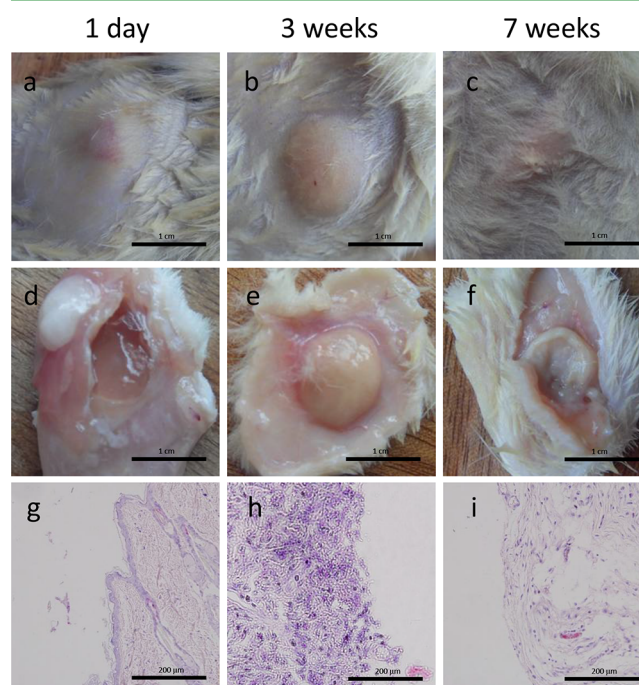


**Figure 8.** The CSMA3/SC3 mixture aqueous solution (0.5 mL, 3 wt %) was subcutaneously injected into rats by a syringe with a 21-gauge needle for 1 day, 3 weeks, and 7 weeks. (a–c) Natural state of the hydrogel after injection (scale bar = 1 cm); (d–f) the rats were sacrificed, and the injection site was carefully cut open (scale bar = 1 cm); (g–i) H&E staining of the dermal tissue surrounding the hydrogel (scale bar = 200  $\mu\text{m}$ ).

shows that a hydrogel with a round protrusion was formed when the CSMA/SC mixture aqueous solution was subcutaneously injected into rats with a syringe needle. No local irritation was observed at the injection site, and no locomotor, clinical, or behavior trouble was observed over the period of the study. Figure 9 shows the diameter of the hydrogel after injection under the skin. From Figures 8 and 9, it can be seen that the diameter of the hydrogel decreased as time passed, indicating its biodegradability. Panels b, c, e, and f in Figure 8 also show the decrease in the hydrogel size. There are several *in vivo* enzymes that can degrade chondroitin sulfate and chitosan. For example, PH-20, hyaluronidase-1, and hyaluronidase-4 can degrade chondroitin sulfate, and lysozyme is specific for chitosan degradation. The hydrogel is therefore subject to enzymatic degradation *in vivo*. As the degradation time of the hydrogel could possibly be matched to that of tissue healing, it can be envisioned to encapsulate a CSMA3/SC3 hydrogel with therapeutic cells to foster tissue reconstruction. For an example aimed at cartilage repair, the hydrogel could be loaded with mesenchymal stem cells.

After 1 day, 3 weeks, and 7 weeks, the rats were sacrificed, and the tissue surrounding the hydrogel was harvested, stained with hematoxylin and eosin, and then processed for histology. Mild inflammatory reactions occurred with leukocyte and fibroblast (dark staining cells) hyperplasia in response to the CSMA3/SC3 hydrogel at both 1 day and 3 weeks (Figure 8g and h). This is

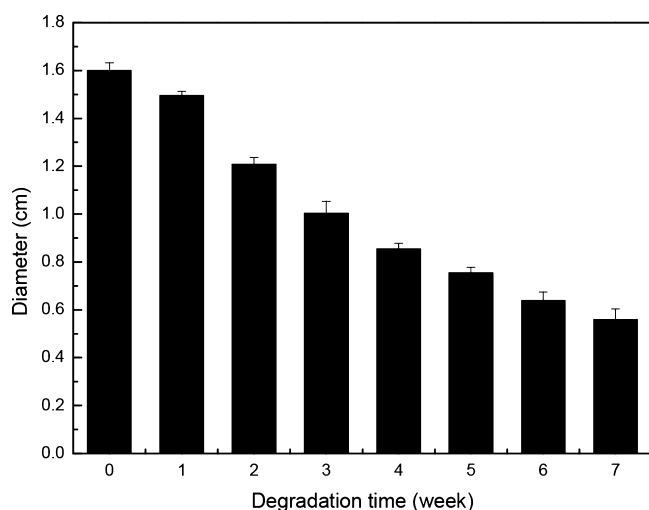


**Figure 9.** In vivo degradation of the injected CSMA3/SC3 hydrogel, showing the transverse diameter as a function of time in which the hydrogel was injected beneath the abdominal skin.

because of a foreign body response. This response, however, seems to diminish with the polymer degradation as the tissue only displays minimal irritation after 7 weeks, as shown in Figure 8f and i. Several overlapping phases were observed in Figure 8i, including the inflammatory, proliferative, and repair phases, which all contribute to tissue repair.<sup>47</sup> An increase in inflammatory leukocytes represents the inflammation phase. The proliferative phase is characterized by the proliferation of neutrophils, macrophages, fibroblasts, and endothelial cells. The repair phase is often initiated by the formation of ECM, which is always accomplished by fibroblasts. After the ECM has been formed, the formation of granulation tissue occurs. Chondroitin sulfate and chitosan have been shown to stimulate cells to migrate, differentiate, proliferate, and produce ECM. Thus, the presence of chondroitin sulfate and chitosan could have contributed to the decreased inflammatory reactions.

## CONCLUSIONS

In this study, we demonstrated the successful modification of chondroitin sulfate and chitosan to form an injectable, self-healing hydrogel. Varying the CSMA to SC ratio affects the cross-linking density of the hydrogels along with their gelation time, water content, and mechanical properties. However, the influence of the CSMA content is dominant for the water content because it is hydrophilic and highly charged. Mechanical properties of the hydrogel under dynamic conditions was determined to mimic dynamic soft tissues. The hydrogel is able to heal autonomously within 2 h. Cells were encapsulated inside the hydrogel, and excellent viability was achieved. Finally, we showed that the hydrogel is biodegradable and produces minimal inflammatory response when injected subcutaneously in a rat model. Additionally, the hydrogel can help in tissue repair. These results demonstrate that the CSMA/SC hydrogel is an ideal candidate as a cell delivery carrier.

## AUTHOR INFORMATION

### Corresponding Authors

\*E-mail: lshy@lzu.edu.cn. Phone: +86-931-8912387. Fax: +86-931-8912582.

\*E-mail: mzliu@lzu.edu.cn.

## Notes

The authors declare no competing financial interest.

## ACKNOWLEDGMENTS

The authors gratefully acknowledge the financial support of the National Natural Science Foundation of China (Grants 51273086, 51473072, and 21202076), the Special Doctoral Program Fund from the Ministry of Education of China (Grant 20130211110017), and the Fundamental Research Funds for the Central Universities (Grant lzujbky-2015-26).

## REFERENCES

- (1) Alvarado-Velez, M.; Pai, S. B.; Bellamkonda, R. V. Hydrogels as Carriers for Stem Cell Transplantation. *IEEE Trans. Biomed. Eng.* **2014**, *61* (5), 1474–1481.
- (2) Vo, T. N.; Kasper, F. K.; Mikos, A. G. Strategies for Controlled Delivery of Growth Factors and Cells for Bone Regeneration. *Adv. Drug Delivery Rev.* **2012**, *64* (12), 1292–1309.
- (3) Kwon, J. S.; Kim, S. W.; Kwon, D. Y.; Park, S. H.; Son, A. R.; Kim, J. H.; Kim, M. S. In Vivo Osteogenic Differentiation of Human Turbinate Mesenchymal Stem Cells in An Injectable in Situ-Forming Hydrogel. *Biomaterials* **2014**, *35* (20), 5337–5346.
- (4) Haines-Butterick, L.; Rajagopal, K.; Branco, M.; Salick, D.; Rughani, R.; Pilarz, M.; Lamm, M. S.; Pochan, D. J.; Schneider, J. P. Controlling Hydrogelation Kinetics by Peptide Design for Three-Dimensional Encapsulation and Injectable Delivery of Cells. *Proc. Natl. Acad. Sci. U.S.A.* **2007**, *104* (19), 7791–7796.
- (5) Merceron, C.; Portron, S.; Masson, M.; Lesoeur, J.; Fellah, B. H.; Gauthier, O.; Geffroy, O.; Weiss, P.; Guicheux, J.; Vinatier, C. The Effect of Two- and Three-Dimensional Cell Culture on the Chondrogenic Potential of Human Adipose-Derived Mesenchymal Stem Cells After Subcutaneous Transplantation with An Injectable Hydrogel. *Cell Transplantation* **2011**, *20* (10), 1575–1588.
- (6) Li, Y.; Rodrigues, J.; Tomas, H. Injectable and Biodegradable Hydrogels: Gelation, Biodegradation and Biomedical Applications. *Chem. Soc. Rev.* **2012**, *41* (6), 2193–2221.
- (7) Balakrishnan, B.; Banerjee, R. Biopolymer-Based Hydrogels for Cartilage Tissue Engineering. *Chem. Rev.* **2011**, *111* (8), 4453–4474.
- (8) Lee, K. Y.; Mooney, D. J. Hydrogels for Tissue Engineering. *Chem. Rev.* **2001**, *101* (7), 1869–1880.
- (9) Yang, J.-A.; Kim, H.; Park, K.; Hahn, S. K. Molecular Design of Hyaluronic Acid Hydrogel Networks for Long-Term Controlled Delivery of Human Growth Hormone. *Soft Matter* **2011**, *7* (3), 868–870.
- (10) Hoare, T. R.; Kohane, D. S. Hydrogels in Drug Delivery: Progress and Challenges. *Polymer* **2008**, *49* (8), 1993–2007.
- (11) Roche, E. T.; Hastings, C. L.; Lewin, S. A.; Shvartsman, D. E.; Brudno, Y.; Vasilyev, N. V.; O'Brien, F. J.; Walsh, C. J.; Duffy, G. P.; Mooney, D. J. Comparison of Biomaterial Delivery Vehicles for Improving Acute Retention of Stem Cells in the Infarcted Heart. *Biomaterials* **2014**, *35* (25), 6850–6858.
- (12) Hoemann, C. D.; Sun, J.; Legare, A.; McKee, M. D.; Buschmann, M. D. Tissue Engineering of Cartilage Using An Injectable and Adhesive Chitosan-Based Cell-Delivery Vehicle. *Osteoarthritis and Cartilage* **2005**, *13* (4), 318–329.
- (13) Frith, J. E.; Cameron, A. R.; Menzies, D. J.; Ghosh, P.; Whitehead, D. L.; Gronthos, S.; Zannettino, A. C. W.; Cooper-White, J. J. An Injectable Hydrogel Incorporating Mesenchymal Precursor Cells and Pentosan Polysulphate for Intervertebral Disc Regeneration. *Biomaterials* **2013**, *34* (37), 9430–9440.
- (14) Kim, Y.-M.; Oh, S. H.; Choi, J.-S.; Lee, S.; Ra, J. C.; Lee, J. H.; Lim, J.-Y. Adipose-Derived Stem Cell-Containing Hyaluronic Acid/Alginate Hydrogel Improves Vocal Fold Wound Healing. *Laryngoscope* **2014**, *124* (3), E64–E72.
- (15) Lü, S.; Li, B.; Ni, B.; Sun, Z.; Liu, M.; Wang, Q. Thermoresponsive Injectable Hydrogel for Three-Dimensional Cell Culture: Chondroitin Sulfate Bioconjugated with Poly(*N*-isopropylacrylamide) Synthesized by RAFT Polymerization. *Soft Matter* **2011**, *7*, 10763–10772.



- (16) Park, K. M.; Lee, S. Y.; Joung, Y. K.; Na, J. S.; Lee, M. C.; Park, K. D. Thermosensitive Chitosan–Pluronic Hydrogel as An Injectable Cell Delivery Carrier for Cartilage Regeneration. *Acta Biomater.* **2009**, *5* (6), 1956–1965.
- (17) Gao, J.; Liu, R.; Wu, J.; Liu, Z.; Li, J.; Zhou, J.; Hao, T.; Wang, Y.; Du, Z.; Duan, C.; Wang, C. The Use of Chitosan Based Hydrogel for Enhancing the Therapeutic Benefits of Adipose-Derived MSCs for Acute Kidney Injury. *Biomaterials* **2012**, *33* (14), 3673–3681.
- (18) Fitzpatrick, S. D.; Jafar Mazumder, M. A.; Lasowski, F.; Fitzpatrick, L. E.; Sheardown, H. PNIPAAm-Grafted-Collagen as An Injectable, In Situ Gelling, Bioactive Cell Delivery Scaffold. *Biomacromolecules* **2010**, *11* (9), 2261–2267.
- (19) Choi, B.; Kim, S.; Lin, B.; Wu, B. M.; Lee, M. Cartilaginous Extracellular Matrix-Modified Chitosan Hydrogels for Cartilage Tissue Engineering. *ACS Appl. Mater. Interfaces* **2014**, *6* (22), 20110–20121.
- (20) Liu, Y.; Cai, S.; Shu, X. Z.; Shelby, J.; Prestwich, G. D. Release of Basic Fibroblast Growth Factor From a Crosslinked Glycosaminoglycan Hydrogel Promotes Wound Healing. *Wound Repair and Regeneration* **2007**, *15* (2), 245–251.
- (21) Kuijpers, A. J.; van Wachem, P. B.; van Luyn, M. J. A.; Brouwer, L. A.; Engbers, G. H. M.; Krijgsveld, J.; Zaat, S. A. J.; Dankert, J.; Feijen, J. In Vitro and In Vivo Evaluation of Gelatin-Chondroitin Sulphate Hydrogels for Controlled Release of Antibacterial Proteins. *Biomaterials* **2000**, *21* (17), 1763–1772.
- (22) Strehin, I.; Nahas, Z.; Arora, K.; Nguyen, T.; Elisseff, J. A Versatile pH Sensitive Chondroitin Sulfate-PEG Tissue Adhesive and Hydrogel. *Biomaterials* **2010**, *31* (10), 2788–2797.
- (23) Bhattarai, N.; Gunn, J.; Zhang, M. Chitosan-Based Hydrogels for Controlled, Localized Drug Delivery. *Adv. Drug Delivery Rev.* **2010**, *62* (1), 83–99.
- (24) Li, Q.; Williams, C. G.; Sun, D. D. N.; Wang, J.; Leong, K.; Elisseff, J. H. Photocrosslinkable Polysaccharides Based on Chondroitin Sulfate. *J. Biomed. Mater. Res., Part A* **2004**, *68A* (1), 28–33.
- (25) Jin, R.; Moreira Teixeira, L. S.; Dijkstra, P. J.; Karperien, M.; van Blitterswijk, C. A.; Zhong, Z. Y.; Feijen, J. Injectable Chitosan-Based Hydrogels for Cartilage Tissue Engineering. *Biomaterials* **2009**, *30* (13), 2544–2551.
- (26) Wiltsey, C.; Christiani, T.; Williams, J.; Scaramazza, J.; Van Sciver, C.; Toomer, K.; Sheehan, J.; Branda, A.; Nitzl, A.; England, E.; Kadlowec, J.; Iftode, C.; Vernengo, J. Thermogelling Bioadhesive Scaffolds for Intervertebral Disk Tissue Engineering: Preliminary In Vitro Comparison of Aldehyde-Based Versus Alginate Microparticle-Mediated Adhesion. *Acta Biomater.* **2015**, *16* (0), 71–80.
- (27) Cao, Y.; Zhang, C.; Shen, W.; Cheng, Z.; Yu, L.; Ping, Q. Poly(*N*-isopropylacrylamide)–Chitosan as Thermosensitive In Situ Gel-Forming System for Ocular Drug Delivery. *J. Controlled Release* **2007**, *120* (3), 186–194.
- (28) Fan, M.; Ma, Y.; Mao, J.; Zhang, Z.; Tan, H. Cytocompatible In Situ Forming Chitosan/Hyaluronan Hydrogels via a Metal-Free Click Chemistry for Soft Tissue Engineering. *Acta Biomater.* **2015**, *20* (0), 60–68.
- (29) Sato, T.; Ebara, M.; Tanaka, S.; Asoh, T.-A.; Kikuchi, A.; Aoyagi, T. Rapid Self-Healable Poly(ethylene glycol) Hydrogels Formed by Selective Metal-Phosphate Interactions. *Phys. Chem. Chem. Phys.* **2013**, *15* (26), 10628–10635.
- (30) Bastings, M. M. C.; Koudstaal, S.; Kieltyka, R. E.; Nakano, Y.; Pape, A. C. H.; Feyen, D. A. M.; van Slochteren, F. J.; Doevendans, P. A.; Sluijter, J. P. G.; Meijer, E. W.; Chamuleau, S. A. J.; Dankers, P. Y. W. A Fast pH-Switchable and Self-Healing Supramolecular Hydrogel Carrier for Guided, Local Catheter Injection in the Infarcted Myocardium. *Adv. Healthcare Mater.* **2014**, *3* (1), 70–78.
- (31) Yang, B.; Zhang, Y.; Zhang, X.; Tao, L.; Li, S.; Wei, Y. Facilely Prepared Inexpensive and Biocompatible Self-Healing Hydrogel: a New Injectable Cell Therapy Carrier. *Polym. Chem.* **2012**, *3* (12), 3235–3238.
- (32) Wei, Z.; Yang, J. H.; Liu, Z. Q.; Xu, F.; Zhou, J. X.; Zrínyi, M.; Osada, Y.; Chen, Y. M. Self-Healing Materials: Novel Biocompatible Polysaccharide-Based Self-Healing Hydrogel. *Adv. Funct. Mater.* **2015**, *25* (9), 1471–1471.
- (33) Lin, L.-J.; Larsson, M.; Liu, D.-M. A Novel Dual-Structure, Self-Healable, Polysaccharide Based Hybrid Nanogel for Biomedical Uses. *Soft Matter* **2011**, *7* (12), 5816–5825.
- (34) Dawlee, S.; Sugandhi, A.; Balakrishnan, B.; Labarre, D.; Jayakrishnan, A. Oxidized Chondroitin Sulfate-Cross-Linked Gelatin Matrixes: a New Class of Hydrogels. *Biomacromolecules* **2005**, *6* (4), 2040–2048.
- (35) Prochazkova, S.; Vårum, K. M.; Ostgaard, K. Quantitative Determination of Chitosans by Ninhydrin. *Carbohydr. Polym.* **1999**, *38* (2), 115–122.
- (36) Ito, T.; Yeo, Y.; Highley, C. B.; Bellas, E.; Benitez, C. A.; Kohane, D. S. The Prevention of Peritoneal Adhesions by In Situ Cross-Linking Hydrogels of Hyaluronic Acid and Cellulose Derivatives. *Biomaterials* **2007**, *28* (6), 975–983.
- (37) Flory, P. J.; Rehner, J. J. Statistical Mechanics of Cross-Linked Polymer Networks II. Swelling. *J. Chem. Phys.* **1943**, *11* (11), 521–526.
- (38) Lee, K. Y.; Bouhadir, K. H.; Mooney, D. J. Degradation Behavior of Covalently Cross-Linked Poly(aldehyde guluronate) Hydrogels. *Macromolecules* **2000**, *33* (1), 97–101.
- (39) Lee, F.; Chung, J. E.; Kurisawa, M. An Injectable Hyaluronic Acid–Tyramine Hydrogel System for Protein Delivery. *J. Controlled Release* **2009**, *134* (3), 186–193.
- (40) Painter, T.; Larsen, B. Formation of Hemiacetals Between Neighbouring Hexuronic Acid Residues During the Periodate Oxidation of Alginate. *Acta Chem. Scand.* **1970**, *24* (3), 813–833.
- (41) Gomez, C. G.; Rinaudo, M.; Villar, M. A. Oxidation of Sodium Alginate and Characterization of the Oxidized Derivatives. *Carbohydr. Polym.* **2007**, *67* (3), 296–304.
- (42) Kang, H.-A.; Jeon, G.-J.; Lee, M.-Y.; Yang, J.-W. Effectiveness Test of Alginate-Derived Polymeric Surfactants. *J. Chem. Technol. Biotechnol.* **2002**, *77* (2), 205–210.
- (43) Tan, H.; Chu, C. R.; Payne, K. A.; Marra, K. G. Injectable In Situ Forming Biodegradable Chitosan-Hyaluronic Acid Based Hydrogels for Cartilage Tissue Engineering. *Biomaterials* **2009**, *30* (13), 2499–2506.
- (44) Roberts, M. C.; Hanson, M. C.; Massey, A. P.; Karren, E. A.; Kiser, P. F. Dynamically Restructuring Hydrogel Networks Formed with Reversible Covalent Crosslinks. *Adv. Mater.* **2007**, *19* (18), 2503–2507.
- (45) Saums, M. K.; Wang, W.; Han, B.; Madhavan, L.; Han, L.; Lee, D.; Wells, R. G. Mechanically and Chemically Tunable Cell Culture System for Studying the Myofibroblast Phenotype. *Langmuir* **2014**, *30* (19), 5481–5487.
- (46) Banerjee, A.; Arha, M.; Choudhary, S.; Ashton, R. S.; Bhatia, S. R.; Schaffer, D. V.; Kane, R. S. The Influence of Hydrogel Modulus on the Proliferation and Differentiation of Encapsulated Neural Stem Cells. *Biomaterials* **2009**, *30* (27), 4695–4699.
- (47) Henderson, E.; Lee, B. H.; Cui, Z.; McLemore, R.; Brandon, T. A.; Vernon, B. L. In Vivo Evaluation of Injectable Thermosensitive Polymer with Time-Dependent LCST. *J. Biomed. Mater. Res., Part A* **2009**, *90A* (4), 1186–1197.